

MORPHOLOGICAL, STRUCTURAL AND OPTICAL CHARACTERISTICS OF GRAPHENE OXIDE LAYERS AND METAL/INTERLAYER/SEMICONDUCTOR PHOTOVOLTAIC DIODE APPLICATION

O. GULLU^{a*} M. ÇANKAYA^b

^aUniversity of Batman, Department of Physics, Bati Raman Campus, Batman, TURKEY

^bUniversity of Erzinçan, Department of Biology, Erzinçan, TURKEY

This work describes the optical, morphological and structural characterizations of graphene oxide (GO) layers grown by drop casting and annealing process. UV-vis optical measurement shows that the values of direct and indirect optical gap energy of the GO film are 3.89 eV and 3.21 eV, respectively. The graphene oxide (GO) layer has been placed in the metal/ interlayer /semiconductor (MIS) diodes (total 17 devices) on p-Si wafers. The graphene oxide diodes give a better barrier height enhancement as compared with the conventional diodes. The value of homogeneous barrier height for Al/GO/p-Si MIS junctions was extracted as 0.74 eV. The diodes were also investigated under 300 watt light illumination for photovoltaic applications. Additionally, interfacial properties of the MIS diode with GO interlayer were determined. It has been seen that the capacitance of the device changes as a function of gate voltage and signal frequency from the capacitance-frequency measurements. It has also been reported that the interfacial trap charges reduce the capacitance with increasing frequency values.

(Received January 9, 2018; Accepted April 19, 2018)

Keywords: Graphene oxide; thin films; Band gap; MIS diode; Schottky barrier

1. Introduction

It is well known that carbon structures as the most common elements in the world are more biologically and environmentally friendly than inorganic compounds for different applications [1]. The human beings have used these materials in daily lives for hundreds of years without critical toxicity issues [2]. Indeed, carbon-based structures are key building blocks for many novel technological applications. In particular, graphene, a two-dimensional single atomic layer of sp² bonded carbon atoms, is a favorable substance due to its unique and exceptional electrical, thermal, and optical features [3]. Graphene oxide (GO) is also a widely investigated valuable novel material, a graphene derivative material with oxygen groups on the carbon bone scaffold of graphene [2,4].

The performance, reliability and stability of metal/semiconductor (MS) and/or metal/interlayer/semiconductor (MIS) junctions are strongly affected by the interfacial layer properties. The electrical parameters of the MS diodes can be changed by means of the choice of suitable interlayer [5]. However, the Schottky barrier height (BH) is restricted to the range of 0.40-0.70 eV for p-Si which is independent of top contact metal. In spite of this, the formation of Schottky contacts with a low ideality factor by using thin interlayers is one of the essential prerequisites for devices [5-8]. Onganer et al. [9] have reported that the barrier height was 0.84 eV from current-voltage (I-V) measurement for metallic polymer/p-Si diode. Recently, Temirci et al. [10] have reported the barrier height value of 0.78 eV and ideality factor value of 1.54 for Cu/Rhodamine-101/p-Si diode. In other study, Karataş et al. [11] have fabricated Al/Rh101/p-Si contact. They found the barrier height of 0.817 eV for the Al/Rh101/p-Si contact. Erdogan and Gullu [12] have recently found as the BH value of 0.64 eV and the ideality factor of 2.39 for the

*Corresponding author: omergullu@gmail.com

Au/CuO/p-Si diode. However, there are many reports on the properties and applications of graphene and graphene oxide in order to improve or modify the electrical performance of silicon contacts compared with other materials [13-35]. An et al. [13] fabricated graphene/p-Si junction devices grown by chemical vapour deposition method of graphene. Important diode parameters, such as the Schottky barrier height (Φ_b), ideality factor (n), and series resistance (R_s), were extracted as 0.47eV, 8.1 and 1.12 k Ω by using forward bias I-V characteristics. Yim et al. [14] fabricated the graphene/n-Si device. The Schottky barrier height and ideality factor of the graphene/n-Si diode were calculated as 0.69 eV and 1.38 by using the I-V characteristics. Phan et al.[35] fabricated Al/GO/n-Si junction by using an interlayer of GO material. The ideality factor and the barrier height of the Al/GO/n-Si device in darkness were as 0.50 and 2.94, respectively. The I-V measurements of the Al/GO/n-Si junction were also performed under different light conditions. It was seen that the Al/GO/n-Si/Al junction was highly sensitive to illumination from the time dependent photocurrent characteristics. They have suggested that the GO-based junction might be handled as a photosensor[35].

The motivation of the present work is to explore some advantages of GO interlayer that can circumvent the problems of conventional Schottky diodes (in this case Al/p-Si diode). Firstly, the optical, morphological and structural features of the GO film formed on glass by the drop casting technique have been examined by using ultraviolet-visible (UV-vis) spectroscopy, atomic force microscopy (AFM), x-ray diffraction method (XRD) and scanning electron microscopy (SEM). The GO interlayer on p-si wafer were formed by using drop casting method to fabricate the junction. The detail direct current (DC) and alternating current (AC) measurements were performed to understand the charge transport mechanism and the interface structure of the GO/p-Si diode. In fact, the role of the GO layer in improving the electrical properties of conventional Al/p-Si diode was investigated in this study. Also, the influence of light illumination on the electronic features of the devices were evaluated for optical sensing applications. The results indicate that the thin layer of graphene oxide acts as a material with good optical sensing.

2. Experimental details

2.1. Preparation of GO films:

All chemicals were of analytical grade and used as purchased. The GO material is prepared by oxidation of graphite with a modified Hummers technique [36,37]. Chemical structure of GO is shown in Fig.1. GO solution was prepared in 1mg/mL concentration in de-ionized water for optical and structural measurements and device applications.

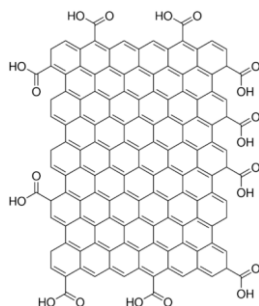


Fig. 1. The chemical structure of GO.

2.2. Optical, morphological and structural measurements of the GO films

GO were coated by drop casting method on glass substrates and then annealed at 100 °C for 30 minutes. The optical absorption characteristic of GO film on the glass slide was performed by using a Shimadzu 3600 UV-vis system between the 190 nm and 1100 nm at room temperature. The XRD characterization experiment was performed by X-ray diffraction (Rigaku 2200D/Max X-Ray diffractometer (45 kV, 40 mA) working with Cu K α radiation of wavelength 1.5406 Å in the

2 θ range from 5° to 50°). The surface morphology of the films were investigated by atomic force microscopy (NanoMagnetics device, Oxford,UK) and a Zeiss Supra 50 VP scanning electron microscope. A Keithley 4200 SCS system was used for electrical characterization at room temperature.

2.3. Production and Electrical characteristics of Al/GO/p-Si junctions

The p-Si (100) wafer was pretreated by ultra-cleaning before coating. The pretreatment consists of (i) cleaning in a solution containing NH₃, H₂O₂, and H₂O in 1:1:6, (ii) dipping in HF solution to remove oxide group and (iii) lastly boiling in a solution containing HCl, H₂O₂, and H₂O in 1:1:6 at 60 °C. The GO dispersion was dropped onto the p-Si wafer with Al ohmic contact. GO thin films were deposited by drop casting technique on p-type Si substrates. After the GO coating, the structure was annealed at 100 °C for 30 min. The circular Al gate with an area of $7.85 \times 10^{-3} \text{ cm}^2$ was then formed by evaporating with the mask on the GO film of the Si wafer. Al film has a thickness of about 100 nm. A reference diode without GO film was also fabricated to present the influence of GO interlayer.

3. Results and discussion

3.1. Optical absorbance features of GO layers

The standard optical transmittance spectrum of the GO film formed on glass slide is shown in Fig. 2. The values of transmittance of the GO film increase with the increasing wavelength and reach to a maximum value of 72.5% at wavelength of 900 nm. This characteristic of the transmittance is similar to that obtained by Wu and Ting [38].

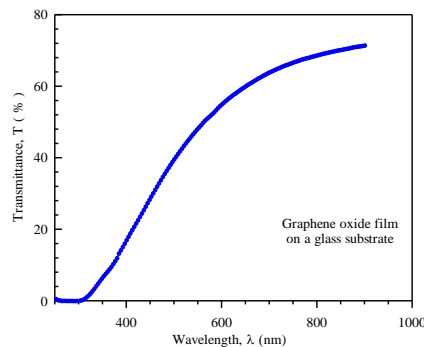


Fig. 2. The standard transmittance characteristic of the GO layer formed on glass slide.

Optical absorbance characteristic of the GO thin layer on the glass slide was investigated by the following relationship,

$$Ah\nu = B(h\nu - E_g)^m, \quad (1)$$

where B is a constant, E_g is the optical band gap of the film, A is optical absorbance of the film. The exponent m depends on the nature of the transition, $m = 1/2$, 2 , $3/2$, or 3 for allowed direct, allowed indirect, forbidden direct or forbidden indirect transitions, respectively. Fig. 3 presents UV-vis characteristic of the GO thin layer on the glass substrate.

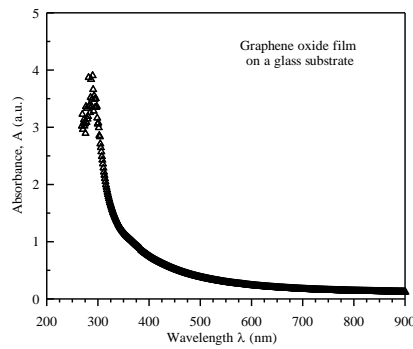


Fig. 3 UV-vis spectrum of the GO thin layer on the glass substrate.

The absorbance spectrum of GO has a peak at about 285 nm that is due to π - π^* transition of aromatic C-C bonds. A “shoulder” at a wavelength of about 350 nm is also present, indicating n- π^* electronic transitions in carbonyl and carboxyl functional groups [39-44]. This absorbance spectrum agrees with some previous works [16,39-44]. Fig. 4 shows the curve of $(Ah\nu)^2$ vs. $h\nu$ extracted from Eq.1 for $m=1/2$. The direct band gap of the GO film was found as 3.89 eV from extrapolation of the linear part of the curve at $(Ah\nu)^2 = 0$. Also, Fig. 5 presents the curve of $(Ah\nu)^{1/2}$ vs. $h\nu$ according to Eq.1 for $m=2$. The indirect band gap of the GO film was calculated as 3.21 eV by using extrapolation of the linear section of the curve at $(Ah\nu)^{1/2} = 0$. These band gap values agree well with those previously found by various researchers. Recently, Velasco-Soto et al. [43] have found that the indirect band gap calculated from Tauc plots was 2.70 eV for GO layers formed at various conditions. Also, Singh et al. [45] reported that the GO film on quartz substrates had a direct optical band gap of 3.20 eV. Chowdhury [46] found that the band gap of GO layers was between 2.10 eV and 2.40 eV. Mathkar et al. [47] have reported an optical band gap of 3.5 eV for the GO films. The our optical band gap energy values are consistent with some previous studies [45-47].

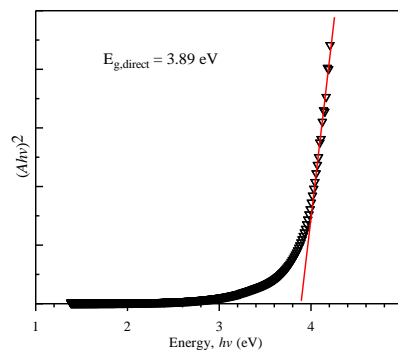


Fig. 4 The curve of $(Ah\nu)^2$ vs. $h\nu$ of the GO thin layer on the glass substrate.

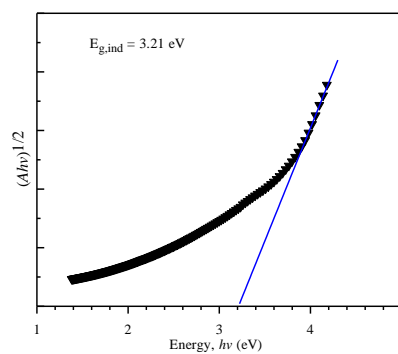


Fig. 5 The curve of $(Ah\nu)^{1/2}$ vs. $h\nu$ of the GO thin layer on the glass substrate.

3.2. Surface Morphology and Structural Investigation of the GO thin layers

The surface morphologies of the drop casting coated GO film on a glass substrate were displayed in SEM and AFM images (Figures 6 and 7). Figure 6 shows the SEM pictures of the GO film on a glass. The surface of GO film is smooth, with many wrinkles as also observed in previously reported graphene oxide sheets [19]. Fig. 7 shows the AFM image of the graphene oxide on a glass substrate. The images were taken in air. Fig. 7 supports the typical folded and wrinkled nature of GO layer. The formation of complete films is desirable for these GO/Si solar cells as it allows holes to travel efficiently throughout the GO layer to the front electrode contact, decreasing the chance of recombination within the film and the need for a hopping transport mechanism. The root mean square (RMS) roughness is 63 nm. Recently, Drewniak et al. [48] have reported that the RMS roughness value from the AFM image for the thin GO layer on the silicon substrate is 28.51 nm, which proves the inhomogeneity of the surface of GO. Also, Timoumi et al. [49] have found have reported that the RMS roughness value of the thin GO layer on the glass substrate is 8.4 nm. The RMS roughness value in the present work is higher than the that of the previously reported studies. This could be attributable to the post-processing procedure, film thickness, coating method/conditions and substrate type (such as glass, mica, silicon) [49]. Furthermore, the higher value of the ideality factor (ideal value is 1) for Schottky diodes is the presence of inhomogeneities of Schottky barrier height and existence of interface states, oxide (native+GO) layer on silicon substrate and series resistance [50]. Also, the main factors limiting the responsivity of the GO/Si Schottky junctions are recombination of the generated electron-hole pairs, particularly at the GO/Si interface, and absorption of photons outside of the depletion region. The responsivity could be increased by improving the interface properties, and optimizing the silicon substrate doping [50].

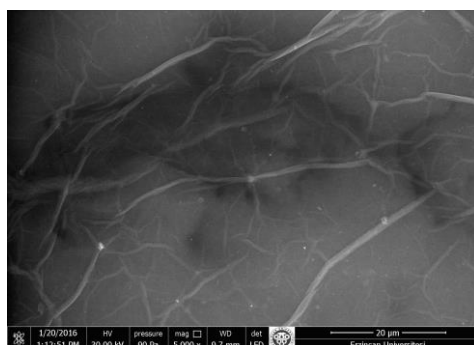


Fig. 6 SEM image of GO thin film on the glass slide.

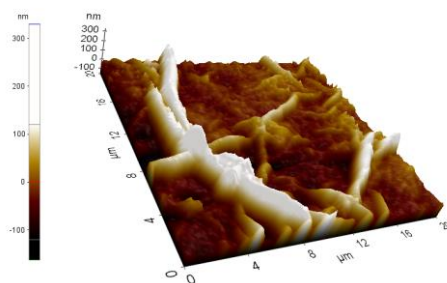


Fig. 7 AFM image of GO thin layer on the glass slide.

The x-ray diffraction pattern of the graphene oxide on the glass is illustrated in Fig. 8. As seen in the XRD pattern, a broad peak near 10.30° was observed. The XRD diffractogram of drop casting coated GO film consists of a single strong diffraction peak at 10.30° (2θ scale) arising

from (001) reflections of GO. The (001) reflection of GO film gives full width at half maximum value of 0.41° . This peak corresponds to the interlayer spacing of 8.58 \AA . Moon et al. [51] have also synthesized graphene oxide using modified Hummer's method and observed a broad peak around 10.27° in the XRD pattern. Our XRD pattern agrees well with those previously presented by various studies [51-54].

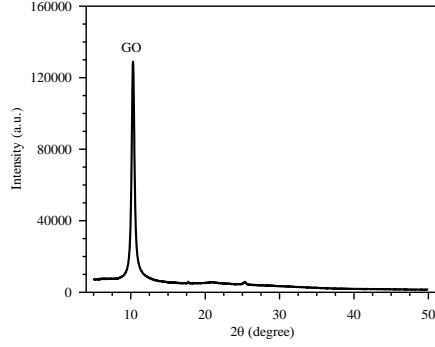


Fig. 8 The XRD pattern of the graphene oxide on the glass.

3.3. The I-V characteristics of the Al/GO/p-Si junctions

The current based on the thermionic emission model as a function of voltage for $qV > 3kT$ in the metal-semiconductor contact is given as [55,56]

$$I = I_0 \exp\left(\frac{qV}{nkT}\right) \quad (2)$$

where V is the gate voltage, n is the ideality factor of the diode and I_0 is the reverse bias leakage current extracted from

$$I_0 = AA^*T^2 \exp\left(-\frac{q\Phi_b}{kT}\right), \quad (3)$$

where A is the contact area, A^* is the Richardson constant of p-Si semiconductor, k is the Boltzmann constant, T is the temperature in Kelvin, q is the charge of electron and Φ_b is the barrier height (BH). The values of n and Φ_b by using Eqs.2 and 3 are presented as:

$$n = \frac{q}{kT} \left(\frac{dV}{d \ln I} \right) \quad (4)$$

and

$$\Phi_b = \frac{kT}{q} \left(\frac{\ln(AA^*T^2)}{I_0} \right), \quad (5)$$

respectively.

Fig. 9 presents the $\ln I$ - V measurements of the Al/GO/p-Si MIS structures (total 17 diodes) fabricated on the same p -type Si wafer. All of the Al/GO/p-Si MIS diodes shown in Fig.9 have good rectifying properties. The $\ln I$ - V plots of the MIS devices have linear regions at low voltage region. But they present a curvature by reason of the influence of series resistance (R_s). The ideality factors n and barrier heights (BHs) Φ_b for each diode are calculated from of the $\ln I$ - V curves by using Eqs. 4 and 5, respectively. Fig. 10 shows the $\ln I$ - V plots of the Al/p-Si control

junction and one of the Al/GO/p-Si MIS diodes. Also, the figure presents that the reverse bias current of the Al/GO/p-Si diode reduces significantly with respect to reverse current of MS control junction. The ideality factor and barrier height for one of the Al/GO/p-Si contacts in dark is extracted as 1.48 and 0.76 eV, respectively. Also, the ideality factor and barrier height of the Al/p-Si reference (control) MS junction are 1.72 and 0.65 eV, respectively. These parameters were given in Table 1. The ideality factor calculated with the image-force influence only can be near 1.01 or 1.02 [57]. Also, the barrier height value of 0.76 eV determined for one of the Al/GO/p-Si contacts is higher than value of 0.65 eV for Al/p-Si reference MS junction shown in Fig. 10.

Table 1. The diode parameters of Al/p-Si control diode and Al/GO/p-Si diode.

Device	I-V		Cheung				Norde	
			dV/dlnI-I		H(I)-I			
	Φ_b (eV)	n	n	R_s (k Ω)	Φ_b (eV)	R_s (k Ω)	Φ_b (eV)	R_s (k Ω)
Al/p-Si	0.65	1.72	5.87	0.60	0.62	1.09	0.69	3.42
Al/GO/p-Si	0.76	1.48	3.42	6.95	0.73	8.67	0.79	40.81

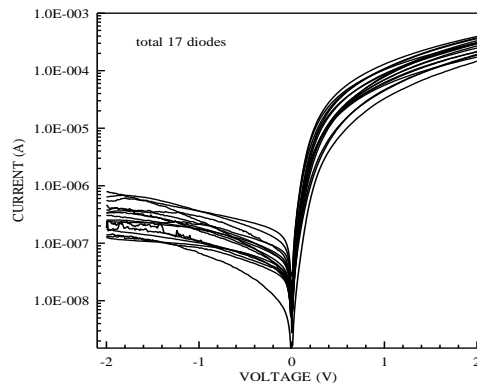


Fig. 9. Current-voltage characteristics of the Al/GO/p-Si Schottky devices (total 17 diodes).

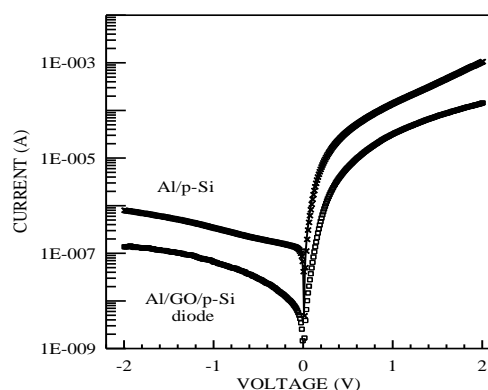


Fig.10. Current-voltage characteristics of one of the Al/GO/p-Si MIS devices and a conventional Al/p-Si MS control junction in dark and at room temperature

In literature, a lot of paper has been presented for the production of MIS contacts by employing the different nano-carbon based materials such as graphene, GO, carbon nanotube (CNT), etc. The results of some workers for the values of Schottky barrier height and ideality factor were given in Table 2. For example, An et al. [13] found as 0.47eV and 8.1 the values of Schottky barrier height and ideality factor for the graphene/p-Si junction. Yim et al [14] also

reported that the Schottky barrier height and ideality factor of the graphene/n-Si diode were calculated as 0.69 eV and 1.38. In other study, Phan et al. [35] fabricated Al/GO/n-Si junction by using an interlayer of graphene oxide (GO) material. The ideality factor and the barrier height of the Al/GO/n-Si device in darkness were as 0.50 and 2.94, respectively. In another study, An et al. [58] fabricated CNT/p-Si junction by using an interlayer of CNT material. The barrier height of the CNT/p-Si device were found as 0.41 eV. In the present study, the GO film creates a physical block between Al metal and the p-Si wafer. GO film could cause to significant change in the energy band structure of MS diode. Thus, the GO interlayer between p-Si wafer and the metal enhances the barrier height of Al/p-Si MS control junction [59]. In conclusion, we have deduced that the electrical features of conventional Al/p-Si junction can be well improved by GO inter-layer film.

Table 2. Some diode parameters of the works published in the literature of graphene, GO and CNT/Si devices

Device	Workers	Φ_b (eV)	n
Graphene/p-Si	An et al. [13]	0.47	8.1
Graphene/n-Si	Yim et al. [14]	0.69	1.38
GO/n-Si	Phan et al. [35]	0.50	2.94
Graphene/n-Si	Li et al. [19]	0.78	1.57
CNT/p-Si	An et al. [58]	0.41	-
Graphene/n-Si	Tongay et al. [26]	0.40-0.60	1.12-1.90

The interfacial regions of MS or MIS diodes are mostly accepted to be uniform and the junctions are evaluated by the barrier heights and ideality factors [57,60-69]. In this study, the values of BH and ideality factor for the Al/GO/p-Si MIS diodes as seen in Fig. 11 range from 0.68 eV to 0.76 eV, and from 1.48 to 1.82, respectively. There is a linear variation between effective barrier heights and ideality factors. Homogeneous barrier height of the Al/GO/p-Si MIS diodes has been determined as 0.74 eV from extrapolation of BH vs. ideality factor plot shown in Fig. 11.

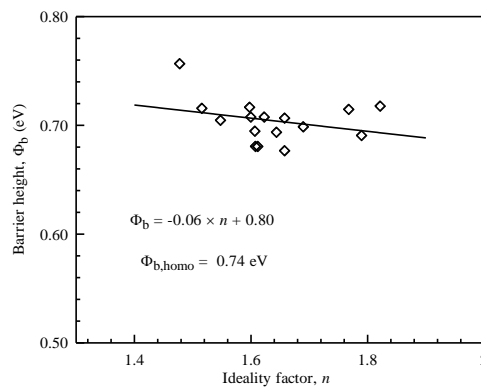


Fig.11. The BH vs. ideality factor plot for the Al/GO/p-Si diodes

Cheung and Cheung [70-72] presented a calculation technique to extract the series resistance values. The I - V characteristic of a junction with the series resistance parameter is given as [72]:

$$I = I_0 \exp \left[\frac{q(V - IR_s)}{nkT} \right]. \quad (6)$$

The series resistance values are extracted from following equations derived from the Eq.(6);

$$\frac{dV}{d(\ln I)} = \frac{nkT}{q} + IR_s, \quad (7)$$

$$H(I) = V - \left(\frac{nkT}{q} \right) \ln \left(\frac{I}{AA^*T^2} \right), \quad (8)$$

and $H(I)$ is expressed as:

$$H(I) = n\Phi_b + IR_s. \quad (9)$$

Fig. 12 and 13 indicate the $\frac{dV}{d(\ln I)}$ vs. I and $H(I)$ - I graphics of the Al/GO/p-Si and the Al/p-Si diodes at room temperature. From the $dV/d(\ln I)$ - I curve, the ideality factor and series resistance of the Al/GO/p-Si diode were found as $n = 3.42$ and $R_s = 6.95 \text{ k}\Omega$, respectively. Also, the ideality factor and series resistance of the Al/p-Si control diode were found as $n = 5.87$ and $R_s = 0.60 \text{ k}\Omega$, respectively. These parameters were given in Table 1. It has been seen that the ideality factor value extracted from the $dV/d(\ln I)$ - I curves is different from the value of n determined from the forward-bias $\ln I$ - V plot. This difference may be ascribed to the existence of the series resistance, interface states and the interfacial layer (GO+native oxide) [73]. However, the $H(I)$ - I plot will be linear [66]. The slope of the plot provides a second extraction way of R_s . The values of barrier height and series resistance for the Al/GO/p-Si diode were found as 0.73 eV and $8.67 \text{ k}\Omega$ by using the $H(I)$ - I curve, respectively. Also, the values of barrier height and series resistance for the Al/p-Si control diode were found as 0.62 eV and $1.09 \text{ k}\Omega$. These parameters were given in Table 1. The increase in the barrier height of the Al/GO/p-Si diode is similar to the evaluation performed in the I-V analysis. However, the GO layer in the Al/GO/p-Si device forms an additional barrier between Al and p-Si and causes to important increase in the series resistance of the diode.

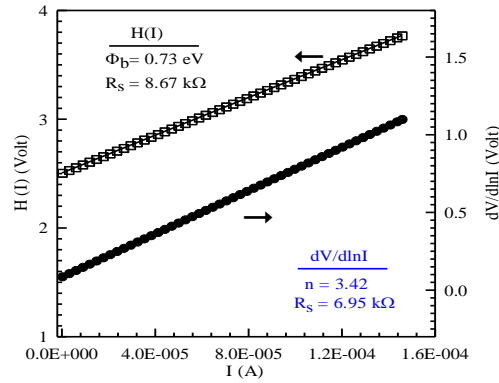


Fig.12. $H(I)$ - I and $dV/d(\ln I)$ - I curves for the Al/GO/p-Si MIS diode.

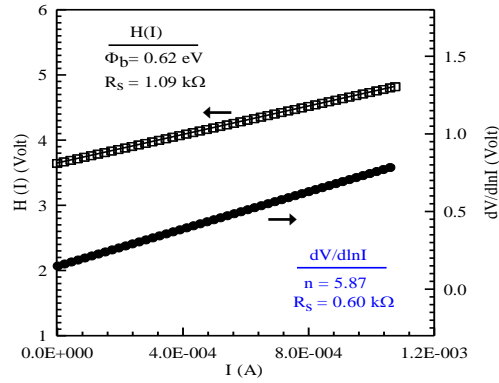


Fig.13. $H(I)$ - I and $dV/d(\ln I)$ - I curves for the Al/p-Si control diode.

To determine the series resistance has recently been proposed a different method by Norde [74]. In the modified Norde's technique, the following function has been given as:

$$F(V) = \frac{V}{\gamma} - \frac{1}{\beta} \ln \left(\frac{I(V)}{AA^*T^2} \right) \quad (10)$$

where $F(V)$ is Norde function, γ is the first integer (dimensionless) greater than n . $I(V)$ is the current found from the I - V measurement and β is a temperature-dependent value extracted by $\beta = q/kT$. The barrier height of the diode can be obtained from Eq. (11),

$$\Phi_b = F(V_0) + \frac{V_0}{\gamma} - \frac{kT}{q} \quad (11)$$

where $F(V_0)$ is the minimum of $F(V)$ - V curve and V_0 is the related voltage value.

Fig. 14 shows the $F(V)$ - V curves of the Al/GO/p-Si junction and Al/p-Si diode. In light of Norde's function, the value of series resistance is given as;

$$R_s = \frac{kT(\gamma - n)}{qI} \quad (12)$$

By using $F(V_0)=0.73$ V and $V_0=0.17$ V values from the F - V curve, the values of barrier height and series resistance for the Al/GO/p-Si MIS diode were found as 0.79 eV and 40.81 k Ω , respectively. However, the values of barrier height and series resistance for the Al/p-Si control diode were extracted as 0.69 eV and 3.42 k Ω , respectively. These parameters were given in Table 1. There is a difference in the Φ_b values determined from the $\ln I$ - V method, Cheung technique and Norde method. Also, the value of series resistance is dramatically higher than that obtained from Cheung functions. Differences in the barrier height and the series resistance values obtained from three methods for the Al/GO/p-Si junction is due to the determinations from different parts of the I - V curve [75]. Cheung functions are only applied to the non-linear region in high voltage region of the forward-bias $\ln I$ - V characteristics. But, Norde's functions are applied to the full forward-bias region of the $\ln I$ - V characteristics of the junctions. Further explanations on the differences were given in our previous study [76].

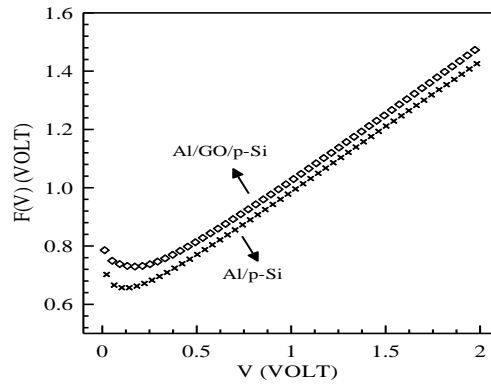


Fig. 14. $F(V)$ - V plots for the Al/GO/p-Si and Al/p-Si diodes.

3.4. Extraction of the interface state density of the Al/GO/p-Si diode

Card and Rhoderick [77] have recently presented a technique to extract the interface state density N_{SS} for a MS diode with interface states. The interface state density N_{SS} is given as:

$$N_{SS} = \frac{1}{q} \left[\frac{\varepsilon_i}{\delta} (n(V) - 1) - \frac{\varepsilon_s}{w} \right] \quad (13)$$

where w is the width of depletion region, ε_s is the permittivity of the semiconductor, ε_i is the permittivity of the interfacial layer, δ is the thickness of interlayer, and $n(V) = \frac{V}{(kT/q) \ln(I/I_0)}$

is the ideality factor as a function of gate voltage. The energy of the interface states (E_{SS}) in the MIS diodes are stated as:

$$E_{SS} - E_V = q\Phi_b - qV \quad (14)$$

The values of $E_{SS} - E_V$ of the interface states has been extracted from the I - V measurement. The curve of N_{SS} vs. $E_{SS} - E_V$ by using Eqs. (13) and (14) has been drawn as seen in Fig. 15. It has been shown that the density of interface states increases with decreasing $E_{SS} - E_V$ values from the Fig. 14. The density of interface states of the Al/GO/p-Si junction varies from $2.47 \times 10^{14} \text{ eV}^{-1} \text{ cm}^{-2}$ to $2.41 \times 10^{13} \text{ eV}^{-1} \text{ cm}^{-2}$. Tozlu et al. [78] have recently reported that the density of interface state for the metal/polymer/p-Si diode with polymer interlayer (polyvinyl phenol (PVP) + poly(melamine-co-formaldehyde) (PMF)) varied from 4.5×10^{12} to $6.5 \times 10^{11} \text{ cm}^{-2} \text{ eV}^{-1}$. Kavasoglu et al. [79] have also presented that the density of interface states for Au/Poly(4-vinyl phenol)/p-Si junction is between $1.5 \times 10^{13} \text{ cm}^{-2} \text{ eV}^{-1}$ and $1.0 \times 10^{12} \text{ cm}^{-2} \text{ eV}^{-1}$. Gullu et al. [80] prepared an Al/Congo Red/p-Si MIS diode with an organic film on p-Si wafer. It was reported that the interface-state density of the MIS diode changed from $1.24 \times 10^{13} \text{ cm}^{-2} \text{ eV}^{-1}$ to $2.44 \times 10^{12} \text{ cm}^{-2} \text{ eV}^{-1}$. Also, Yakuphanoglu et al [59] showed that the density of interface states for the Al/CoPc/p-Si junction changed from $1.23 \times 10^{14} \text{ cm}^{-2} \text{ eV}^{-1}$ to $6.90 \times 10^{13} \text{ cm}^{-2} \text{ eV}^{-1}$. Erdogan and Gullu [81] have recently investigated the structural morphological and optical characteristics of the Cr_2O_3 films coated on p-Si wafers by using the sol-gel technique. They have also examined the I - V measurements of the Au/ Cr_2O_3 /p-Si diode. They [81] have indicated that the interface state density of the Au/ Cr_2O_3 /p-Si junction is in the range of $2.90 \times 10^{13} \text{ eV}^{-1} \text{ cm}^{-2}$ - $8.45 \times 10^{12} \text{ eV}^{-1} \text{ cm}^{-2}$. In the present work, the density of interface states extracted for the Al/GO/p-Si device is in well agreement with the results of previously presented studies. The GO thin interlayer film modifies the semiconductor substrate surfaces, and then the chemical interaction at the interface between Al and p-Si wafer due to the effect of native oxide+GO interfacial layer will cause to new states [59,79,82-83].

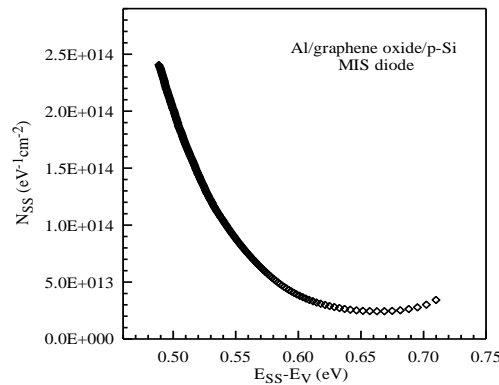


Fig. 15. N_{SS} vs. $(E_{SS}-E_V)$ plot of the Al/GO/p-Si MIS device.

3.5. Photovoltaic properties of the Al/GO/p-Si MIS diode

The influence of 300 watt light illumination on the Al/GO/p-Si junction is presented in Fig. 16. The current of the junction under light illumination is higher than that in the dark. The light illumination causes to the production of new electron-hole pairs [39]. The charge carrier creation is correlated with the difference in electron affinity between p-Si and the GO. The diode indicated photovoltaic feature with a maximum open-circuit voltage of $V_{oc} = 100$ mV, a short-circuit current of $I_{sc} = 0.77$ μ A, a fill factor $FF = 0.33$ and a power conversion efficiency (PCE) of $\eta = 0.0029\%$ under light illumination of 300 watt. However, it is worth noting that this PCE value is still lower than conventional silicon p-n or Schottky junction photodetectors. This could be due to defects and traps at the GO/p-Si interface introduced during the fabrication process due to the drop cast method [13]. The interfacial (native oxide+GO) layer could also be a contributing factor to the low PCE [13,84]. This implies that the PCE of the graphene/Si Schottky junction photodetectors could be improved by further optimizing and controlling the processing and fabrication conditions.

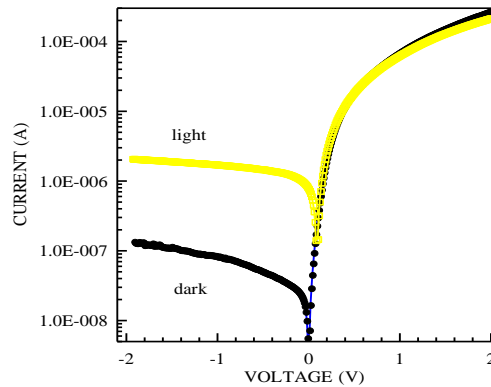


Fig.16. The dark and light I-V measurements of one of the Al/GO/p-Si MIS devices.

3.6. Analysis of Capacitance-Conductance-Frequency (C-G-f) Characteristics of the Al/GO/p-Si junction

The capacitance-voltage (C-V) measurement can present important information about the interfacial properties of the diodes. Figs. 17 and 18 show the measured capacitance (C) and conductance (G) of the Al/GO/p-Si diode as a function of the frequency (f) with steps of 0.04 V, respectively. The capacitance values increases with a decreasing in the frequency range of 3 kHz - 10 MHz as shown in Fig. 16.

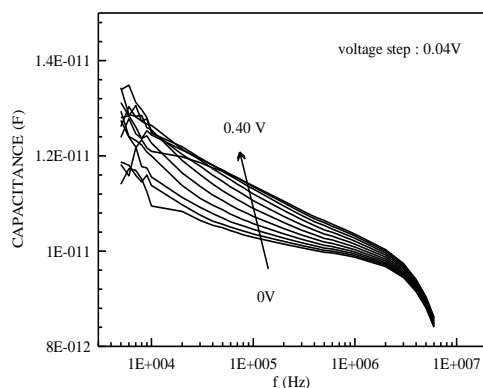


Fig.17. Capacitance-frequency (C - f) measurements of the Al/GO/p-Si MIS junction as a function of voltage

As seen in Fig.18, the measured conductance as a function of frequency increases with the increasing voltage. This situation is attributed to the presence of a continuous distribution of the interface states, causing to a clear decrease of the reaction of the interface states to the applied alternative voltage [85,86]. The values of capacitance and conductance of a junction generally depend on the voltage and frequency of applied alternative signal due to the particular features, such as impurity level of the semiconductor, high series resistance, etc. At low frequency region, the diode capacitance is influenced by the depletion capacitance of the junction. If the signal frequency increases, the total junction capacitance is dominated not only by the depletion capacitance but also by the bulk resistance and related with hole or electron emission from deep impurity levels [55,85,86].

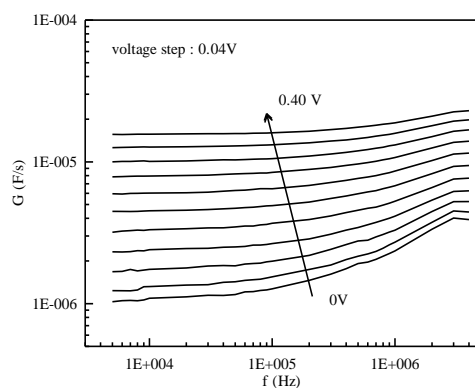


Fig.18. Conductance-frequency (G - f) measurements of the Al/GO/p-Si MIS diode for various voltages

4. Conclusions

In conclusion, the surface morphology, optical absorbance, and structural features of the GO films were examined by using the UV-vis method, AFM, XRD and SEM. The GO layer is smooth, with many wrinkles as also observed in previously reported graphene oxide sheets. The optical absorbance spectrum of GO film has a peak at about 285 nm that is due to π - π^* transition of aromatic C-C bonds. A “shoulder” at a wavelength of about 350 nm is also present, indicating n - π^* electronic transitions in carbonyl and carboxyl functional groups. The values of direct and indirect band gap of the GO film were found as 3.89 eV and 3.21 eV, respectively. Also, the Al/GO/p-Si junctions have been formed on the p-Si wafer. Electrical characteristics of the diodes were investigated by using I-V and C-G-f measurements. In this work, the values of BH and ideality factor for the Al/GO/p-Si MIS junctions range from 0.68 eV to 0.76 eV, and from 1.48 to

1.82, respectively. Homogeneous barrier height of the Al/GO/p-Si MIS diodes was calculated as 0.74 eV. The distribution of interfacial states of the the Al/GO/p-Si junctions has been examined. The density of interface states of the Al/GO/p-Si junction varies from $2.47 \times 10^{14} \text{ eV}^{-1} \text{ cm}^{-2}$ to $2.41 \times 10^{13} \text{ eV}^{-1} \text{ cm}^{-2}$. It was investigated the illumination influence on the electrical features of the junction. The diode indicated photovoltaic feature with $V_{oc} = 100 \text{ mV}$, $I_{sc} = 0.77 \text{ } \mu\text{A}$, $\text{FF} = 0.33$ and $\eta = 0.0029\%$ under light illumination of 300 watt. The results show that GO layer acts as a material with good optical sensing. Our results provide important insights for the future integration of graphene based materials into existing semiconductor technologies.

Acknowledgments

This study is supported by Republic of Turkey-Prime Ministry State Planning organization (DPT) (Project Number: 2010K120610, Batman University Central Research Laboratory).

References

- [1] V. Snitka, J. Nanomed. Res. **2**, 00035 (2015).
- [2] C. Chung, Y.K. Kim, D. Shin, S.R. Ryoo, B.H. Hong, D.H. Min, Acc. Chem. Res. **46**, 2211 (2013).
- [3] N. Rafiq, M. Junaid, A. W. Anwar, Journal of Ovonic Research **13**(4), 195 (2017).
- [4] Y. Zhu, S. Murali, W. Cai, X. Li, J.W. Suk, J.R. Potts, R.S. Ruoff, Adv. Mater. **22**, 3906 (2010).
- [5] S.R. Forrest, M.L. Kaplan, P.H. Schmidt, W.L. Feldmann, E. Yanowski, J. Appl. Phys. **41**, 90 (1982).
- [6] P.L. Hanselaer, W.H. Laflere, R.L. Van Meirhaeghe, F. Cardon, J. Appl. Phys. **56**, 2309 (1984).
- [7] S. Ashok, K. Giewont, IEEE Electron. Dev. Lett. **6**, 462 (1985).
- [8] C. Temirci, B. Bati, M. Saglam, A. Turut, Applied Surface Science **172**, 1 (2001).
- [9] Y. Onganer, M. Saglam, A. Turut, H. Efeoglu, S. Tuzemen, Solid State Electron. **39**, 677 (1996).
- [10] C. Temirci, M. Çakar, Physica B **348**, 454 (2004).
- [11] Ş. Karatas, C. Temirci, M. Çakar, A. Türüt, Appl. Surf. Sci. **252**, 2209 (2006).
- [12] I. Y. Erdogan and O. Gullu, Journal of Alloys and Compounds **492**, 378 (2010).
- [13] Y. An, A. Behnam, E. Pop, G. Bosman, A. Ural, Journal of Applied Physics **118**, 114307 (2015).
- [14] C.Y. Yim, N. McEvoy, G. S. Duesberg, Applied Physics Letters **103**, 193106 (2013).
- [15] D.-T. Phan, G-S Chung, Sensors and Actuators B: Chemical **220**, 1050 (2015).
- [16] S. Rani, M. Kumar, R. Kumar, D. Kumar, S. Sharma, G. Singh, Materials Research Bulletin **60**, 143 (2014).
- [17] S. Rani, M. Kumar, D. Kumar, S. Sharma, Thin Solid Films **585**, 13 (2015).
- [18] T.T. Feng, D. Xie, Y. Lin, YY Zang, TL Ren, R Song, HM Zhao, H Tian, X. Li, H.W. Zhu, L. Liu, Appl. Phys. Lett. **99**, 233505 (2011).
- [19] X. Li, H. Zhu, K. Wang, A. Cao, J. Wei, C. Li, Y. Jia, Z. Li, X. Li, D. Wu, Adv. Mater. **22**, 2743 (2010).
- [20] L. J. Larsen, C. J. Shearer, A. V. Ellis, J. G. Shapter, RSC Adv. **5**, 38851 (2015).
- [21] Z. Tang, Q. Liu, I. Khatri, R. Ishikawa, K. Ueno, H. Shirai, Phys. Status Solidi C **9**, 2075 (2012).
- [22] Z. Zhang, T.X Cui, R.T Lv, H.W. Zhu, K.L. Wang, D. Wu, F. Kang, Journal of nanomaterials **2014**, 359305 (2014).
- [23] K. Ihm, J.T. Lim, K.J. Lee, J.W. Kwon, T.H. Kang, S. Chung, S. Bae, J.H. Kim, B.H. Hong, G.Y. Yeom, Appl. Phys. Lett. **97**, 032113 (2010).
- [24] X. Z. Zhang, C. Xie J.S. Jie, X.W. Zhang, Y. Wu, W.J. Zhang, J. Mater. Chem. A **1**, 6593 (2013).

- [25] K.F. Mak, M.Y. Sfeir, Y. Wu, C.H. Lui, J.A. Misewich, T.F. Heinz, *Phys. Rev. Lett.* **101**, 196405 (2008).
- [26] S. Tongay, T. Schumann, X. Miao, B.R. Appleton, A.F. Hebard, *Carbon* **49**, 2033 (2011).
- [27] C.C. Chen, M. Aykol, C.C. Chang, A.F.J. Levi, S.B. Cronin, *Nano Lett.* **11**, 1863 (2011)
- [28] L. Lancellotti, T. Polichetti, F. Ricciardella, O. Tari, S. Gnanapragasam, S. Daliento, G. Di Francia, *Thin Solid Films* **522**, 390 (2012).
- [29] D. R. Dreyer, S. Park, C. W. Bielawski, R. S. Ruoff, *Chem. Soc. Rev.* **39**, 228 (2010).
- [30] S. Park, R. S. Ruoff, *Nat. Nanotechnol.* **4**, 217 (2009).
- [31] H.J. Zhong, K. Xu, Z.H. Liu, G. Z. Xu, L. Shi, Y.M. Fan, J.F. Wang, G.Q. Ren, H. Yang, *J. Appl. Phys.* **115**, 013701 (2014).
- [32] D. Tomer, S. Rajput, L. J. Hudy, C. H. Li, L. Li, *Nanotechnology* **26**, 215702 (2015)
- [33] D. Tomer, S. Rajput, L. J. Hudy, C. H. Li, L. Li, *Appl. Phys. Lett.* **105**, 021607 (2014).
- [34] S. Rajput, M. Chen, Y. Liu, Y.Y. Li, M. Weinert, L. Li, *Nat. Commun.* **4**, 2752 (2013).
- [35] D.T. Phan, R.K. Gupta, G.S. Chung, A.A. Al-Ghamdi, O. A. Al-Hartomy, F. El-Tantawy, F. Yakuphanoglu, *Solar Energy* **86**, 2961 (2012).
- [36] W. S. Hummers, R. E. Offeman, *J. Am. Chem. Soc.* **80**, 1339 (1958).
- [37] Z. F. Liu, Q. Liu, X.Y. Zhang, Y. Huang, Y.F. Ma, S.G. Yin, Y.S. Chen, *Adv. Mater.* **20**, 3924 (2008).
- [38] T.T. Wu, J.M. Ting, *Surface & Coatings Tech.* **231**, 487 (2013).
- [39] C. P. Liu, Y. Y. Hui, Z. H. Chen, J. G. Ren, Y. Zhou, L. Tang, Y. B. Tang, J. A. Zapien, S.P. Lau, *RSC Adv.* **3**, 17918 (2013).
- [40] I. Karteri, S. Karatas, F. Yakuphanoglu, *Appl. Surf. Sci.* **318**, 74 (2014).
- [41] F. T. Thema, M. J. Moloto, E. D. Dikio, N. N. Nyangiwe, L. Kotsedi, M. Maaza, M. Khenfouch, *Journal of Chemistry* **2013**, 150536 (2013).
- [42] X. Lv, Y. Huang, Z. Liu, J. G. Tian, Y. Wang, Y.F. Ma, J.J. Liang, S.P. Fu, X.J. Wan, Y.S. Chen, *Small* **5**, 1682 (2009).
- [43] M.A. Velasco-Soto, S.A. Perez-Garcia, J. Alvarez-Quintana, Y. Cao, L. Nyborg, L. Licea-Jimenez, *Carbon* **93**, 967 (2015).
- [44] D. C. Marcano, D. V. Kosynkin, J. M. Berlin, A. Sinitskii, Z. Z Sun, A. Slesarev, L. B. Alemany, W. Lu, J. M. Tour, *ACS Nano* **4**, 4806 (2010).
- [45] M. Singh, A. Yadav, S. Kumar, P. Agarwal, *Appl. Surf. Sci.* **326**, 236 (2015).
- [46] F. A. Chowdhury, T. Morisaki, J. Otsuki, M. S. Alam, *Appl. Surf. Sci.* **259**, 460 (2012).
- [47] A. Mathkar, D. Tozier, P. Cox, P. Ong, C. Galande, K. Balakrishnan, A. L. M. Reddy, P. M. Ajayan, *J. Phys. Chem. Lett.* **3**, 986 (2012).
- [48] S. Drewniak, R. Muzyka, A. Stolarczyk, T. Pustelny, M. Kotyczka-Moranska, M. Setkiewicz, *Sensors* **16**, 103 (2016).
- [49] A. Timoumi, M.K. Al Turkestani, J. Ouerfelli, *International Journal of Science and Research* **5**, 1322 (2016).
- [50] O.A. Al-Hartomy, R.K. Gupta, A.A. Al-Ghamdi, F. Yakuphanoglu, *Synthetic Metals* **195**, 217 (2014).
- [51] I. K. Moon, J. Lee, R.S. Ruoff, H. Lee, *Nat. Communications* **1**, 73 (2010).
- [52] S. Bykkam, V. R Kalagadda, S. C. Chidurala and T. Thunugunta, *Int. Journal of Adv. Biotechnology and Research* **4**, 142 (2013).
- [53] G.H. Xu, N. Wang, J.Y. Wei, L.L. Lv, J. Zhang, Z. Chen, Q. Xu, *Ind. Eng. Chem. Res.* **51**, 14390 (2012).
- [54] R.K. Gupta, Z.A. Al-ahmed, F. Yakuphanoglu, *Materials Letters* **112**, 75 (2013).
- [55] E.H. Rhoderick, R.H. Williams, *Metal–Semiconductor Contacts* (second ed.), Clarendon, Oxford, 1988.
- [56] S.M. Sze, *Physics of semiconductor devices* (Second ed.), Wiley, New York, 1981.
- [57] R.F. Schmitsdorf, T.U. Kampen, W. Monch, *J. Vac. Sci. Technol. B* **15**, 1221 (1997).
- [58] Y. An, H. Rao, G. Bosman, A. Ural *J. Vac. Sci. Technol. B* **30**, 021805 (2012).
- [59] F. Yakuphanoglu, M. Kandaz, B.F. Senkal, *Thin Solid Films* **516**, 8793 (2008).
- [60] W. Monch, *J. Vac. Sci. Technol. B* **17**, 1867 (1999).
- [61] R. T. Tung, *Phys. Rev. B* **45**, 13509 (1992).
- [62] Y.P. Song, R.L. Van Meirhaeghe, W.H. Laflere, F. Cardon, *Solid-State Electron.*

- 29**, 633 (1986).
- [63] J.H. Werner, H.H. Guttler, *J. Appl. Phys.* **69**, 1522 (1991).
- [64] J.P. Sullivan, R.T. Tung, M.R. Pinto, W.R. Graham, *J. Appl. Phys.* **70**, 7403 (1991).
- [65] M. Biber, O. Gullu, S. Forment, R.L. Van Meirhaeghe, A. Turut, *Semicond. Sci. Technol.* **21** 1 (2006).
- [66] H. Cetin, B. Sahin, E. Ayyildiz, A. Turut, *Physica B* **364**, 133 (2005).
- [67] Ö. Güllü, S. Asubay, Ş. Aydoğan, A. Türüt, *Physica E* **42**, 1411 (2010).
- [68] U. Rau, H.H. Guttler, J.H. Werner, *Mater. Res. Soc. Symp. Proc.* **260**, 245 (1992).
- [69] C. Detavernier, R.L. Van Meirhaeghe, R. Donaton, K. Maex, F. Cardon, *J. Appl. Phys.* **84**, 3226 (1998).
- [70] S. Aydogan, M. Saglam, A. Turut, *Microelectron. Eng.* **85**, 278 (2008).
- [71] A. Turut, M. Saglam, H. Efeoglu, N. Yalcin, M. Yildirim, B. Abay, *Physica B* **205**, 41 (1995).
- [72] S.K. Cheung, N.W. Cheung, *Appl. Phys. Lett.* **49**, 85 (1986).
- [73] T. Kilicoglu, *Thin Solid Films* **516**, 967 (2008).
- [74] S. Karatas, S. Altindal, A. Turut, M. Cakar, *Physica B* **392**, 43 (2007).
- [75] O. Gullu, S. Aydogan, A. Turut, *Microelectron. Eng.* **85**, 1647 (2008).
- [76] O. Gullu, S. Aydogan, M. Biber, A. Turut, *Vacuum* **82**, 1264 (2008).
- [77] H.C. Card, E.H. Rhoderick, *J. Phys. D* **4**, 1589 (1971).
- [78] C. Tozlu, A. Mutlu, *Synthetic Metals* **211**, 99 (2016).
- [79] N. Kavasoglu, C. Tozlu, O. Pakma, A. S. Kavasoglu, S. Ozden, B. Metin, O. Birgi, S. Oktik, *Synthetic Metals* **159**, 1880 (2009).
- [80] Ö. Güllü, T. Kilicoglu, A. Turut, *Journal of Physics and Chemistry of Solids* **71**, 351 (2010).
- [81] I.Y. Erdogan, O. Gullu, *Appl. Surf. Sci.* **256**, 4185 (2010).
- [82] T.U. Kampen, S. Park, D.R.T. Zahn, *Appl. Surf. Sci.* **190**, 461 (2002).
- [83] S.R. Forrest, M.L. Kaplan, P.H. Schmidt, *J. Appl. Phys.* **60**, 2406 (1986).
- [84] M.C. Putnam, D.B. Turner-Evans, M.D. Kelzenberg, S.W. Boettcher, N.S. Lewis, H. A. Atwater, *Appl. Phys. Lett.* **95**, 163116 (2009).
- [85] C.R. Crowell, K. Nakano, *Solid State Electron.* **15**, 605 (1972).
- [86] S. Aydogan, M. Saglam, A. Turut, *Polymer* **46**, 6148 (2005).